Title: Parsing multiomics landscape of activated synovial fibroblasts highlights drug targets linked to genetic risk of rheumatoid arthritis

Authors: Haruka Tsuchiya[1,†], Mineto Ota[1,2,3,†], Shuji Sumitomo[1], Kazuyoshi Ishigaki[4], Akari Suzuki[3], Toyonori Sakata[5], Yumi Tsuchida[1], Hiroshi Inui[8], Jun Hirose[8], Yuta Kochi[3,6], Yuho Kadono[7], Katsuhiko Shirahige[5], Sakae Tanaka[8], Kazuhiko Yamamoto[3], Keishi Fujio[1,*]

Affiliations:

[1]Department of Allergy and Rheumatology, Graduate School of Medicine, The University of Tokyo, Tokyo, 113-0033, Japan.

[2]Department of Functional Genomics and Immunological Diseases, Graduate School of Medicine, The University of Tokyo, Tokyo, 113-0033, Japan.

[3]Laboratory for Autoimmune Diseases, RIKEN Center for Integrative Medical Sciences, Yokohama, 230-0045, Japan.

[4]Divisions of Genetics and Rheumatology, Department of Medicine, Brigham and Women's Hospital, Harvard Medical School, Boston, MA 02115, USA.

[5]Laboratory of Genome Structure and Function, Institute for Quantitative Biosciences, The University of Tokyo, Tokyo, 113-0032, Japan.

[6]Department of Genomic Function and Diversity, Medical Research Institute, Tokyo Medical and Dental University, Tokyo, 113-8510, Japan.

[7]Department of Orthopaedic Surgery, Saitama Medical University, Saitama, 350-0495, Japan.

[8]Department of Orthopaedic Surgery, Graduate School of Medicine, The University of Tokyo, Tokyo, 113-0033, Japan.

†These authors contributed equally

*Correspondence: K.F., kfujio-tky@umin.ac.jp

Word count:

2925 words

Abstract:

Objectives Synovial fibroblasts (SFs) produce a variety of pathogenic molecules in the inflamed synovium of rheumatoid arthritis (RA). We aimed to gain insight into the pathogenic mechanisms of SFs through elucidating the genetic contribution to molecular regulatory networks under inflammatory condition.

Methods SFs from RA and osteoarthritis (OA) patients (n=30 each) were stimulated with 8 different cytokines (IFN-α, IFN-γ, TNF-α, IL-1β, IL-6/sIL-6R, IL-17, TGF-β1, IL-18) or a combination of all

8 (8-mix). Peripheral blood mononuclear cells (PBMCs) from the same patients were fractioned into five major immune cell subsets ($CD4^+$ T cells, $CD8^+$ T cells, B cells, NK cells, monocytes). Integrative analyses including mRNA expression, histone modifications (H3K27ac, H3K4me1, H3K4me3), 3D genome architecture and genetic variations of SNPs were performed.

Results SFs exposed to synergistically acting cytokines produced markedly higher levels of pathogenic molecules, including CD40 whose expression was significantly affected by a RA risk SNP (rs6074022). Upon chromatin remodeling in activated SFs, RA risk loci were enriched in clusters of enhancers (super-enhancers; SEs) induced by synergistic proinflammatory cytokines. A RA risk SNP (rs28411362), located in a SE under synergistically acting cytokines, formed three-dimensional contact with the promoter of *MTF1* gene, whose binding motif showed significant enrichment in stimulation specific-SEs. Consistently, inhibition of MTF1 suppressed cytokine and chemokine production from SFs and ameliorated mice model of arthritis.

Conclusions Our findings established the dynamic landscape of activated SFs, and yielded potential therapeutic targets associated with genetic risk of RA.

Keywords:

Rheumatoid arthritis, synovial fibroblasts, cytokine synergy, integrative analysis, MTF1

Key messages:

What is already known about this subject?

・In rheumatoid arthritis (RA), a variety of dysregulated molecules from immune cells and mesenchymal cells drive disease progression. Synovial fibroblasts (SFs), the most abundant resident mesenchymal cells in the inflamed synovium, produce a variety of pathogenic molecules including IL-6.

・Genome-wide association studies (GWAS) have identified more than 100 RA susceptibility loci. To gain insight into the pathogenic mechanisms of SFs, understanding the genetic contribution to molecular regulatory networks under inflammatory condition is crucial.

What does this study add?

・Integrated analyses of activated SFs demonstrated that SFs exposed to synergistically acting cytokines produced markedly higher levels of pathogenic molecules. Some of which were significantly affected by RA risk loci in a stimulation-specific manner.

・Chromatin remodeling induced by synergistic proinflammatory cytokines were associated with RA heritability. Some transcription factors (MTF1, RUNX1) could be crucial for this structural rearrangement and the formation of inflammatory arthritis.

How might this impact on clinical practice or future developments?

・Our findings established the dynamic landscape of activated SFs, and yielded potential therapeutic targets associated with genetic risk of RA.

[Main Text:]

Introduction

Rheumatoid arthritis (RA) causes persistent synovitis leading to disabling joint destruction. Current treatment strategies that target cytokines (e.g., TNF-α, IL-6), cell surface proteins (e.g., CD20, CD80/86) or signaling molecules (e.g., Janus kinase) have brought a paradigm shift in RA treatment. However, achieving sustained remission is still challenging even with such agents.[1] Although the concepts of targeting multiple molecules have been proposed, combination or bispecific antibodies (anti-TNF-α and anti-IL-1β or anti-IL-17) failed to improve therapeutic efficacy.[2] These findings imply that some unknown factors play critical roles in the progression of synovitis.

In the pathogenesis of RA, the activities of a variety of dysregulated molecules in immune cells and mesenchymal cells are orchestrated by genetic and environmental factors.[3] To date, more than 100 RA susceptibility loci have been identified in genome-wide association studies (GWAS).[4] Recent genetic studies of autoimmune diseases have reported that the majority (> 90%) of these risk variants are located in non-coding regions and regulate gene expression in a cell type-specific manner,[5] partly in an environment-specific fashion.[6] An integrated understanding of the risk variants' contribution to gene regulatory networks is crucial to gain insight into the pathogenic mechanisms of RA.

Synovial fibroblasts (SFs), the most abundant resident mesenchymal cells in the synovium, are major local effectors in the initiation and perpetuation of destructive joint inflammation through their

production of a variety of pathogenic molecules including IL-6.[3] Previous multiomics data of unstimulated SFs have proposed activated pathways in RASFs.[7] However a comprehensive picture of SFs' contribution to RA pathogenesis has largely remained elusive, perhaps due to their complex features that mutate in response to the proinflammatory milieu.[8] To date, a number of single cytokines that induce the inflammatory behavior of SFs have been reported (e.g., IFN-γ and IL-17 from T cells and TNF-α, IL-1β, IFN-α, IL-18 and TGF-β1 from monocytes).[9] To make matters more complicated, in *in vivo*, SFs are expected to be exposed to a more complex environment. Data show that some cytokine combinations (e.g., TNF-α and IL-17) synergistically enhance the expression of cytokines and chemokines.[10] Those findings emphasize the need to analyze the mechanisms underlying the accelerated inflammatory behavior of SFs in the presence of synergistic factors.

Here, we used integrative methods to analyze genomic, transcriptomic and epigenomic features of RASFs in the presence of various proinflammatory cytokines in RA joints.[11] We demonstrate that SFs exposed to synergistic proinflammatory cytokines show distinct transcriptomic features characterized by elevated expression of pathogenic molecules accompanied by chromatin remodeling associated with genetic risk of RA.

Materials and methods

See online supplementary materials and methods.

Results

Cytokine mixture induce a distinctive transcriptome signature in SFs

We stimulated SFs from RA and osteoarthritis (OA) patients (n=30 each) with 8 different cytokines (IFN-α, IFN-γ, TNF-α, IL-1β, IL-6/sIL-6R, IL-17, TGF-β1, IL-18) or a combination of all 8 (8-mix). We also fractionated peripheral blood mononuclear cells (PBMCs) from the same patients into five major immune cell subsets ($CD4^+$ T cells, $CD8^+$ T cells, B cells, NK cells, monocytes) (figure 1).

First, we compared transcriptomes of SFs between the 10 stimulatory conditions and the 2 diseases. Principal component analysis (PCA) showed that the 8-mix induced a distinct signature compared with the other stimulations, corresponding to the first component (PC1 in figure 2A,B). For instance, the markedly high expression of *IL6* (Primary component loading on PC1 = -0.76, PC2 = 0.26) and other pathogenic genes (e.g., *MMP3*, *CSF2*) was achieved by the 8-mix (figure 2C). On the other hand, RASFs showed different signatures from OASFs irrespective of the stimulations, corresponding largely to the second component (PC2 in figure 2A,B).

Recently, Fan Zhang and colleagues reported that SFs could be clustered into 4 fractions (F1-F4) by single-cell transcriptomics of synovial cells.[12] To elucidate the association between transcriptional changes of activated SFs and those 4 fractions, we scored our samples utilizing the reported gene sets that were characteristic of each of the fractions (online supplementary figure 1). [13] Interestingly, the

F4 score, which was the population abundant in the lining of OA synovium,[12] was higher in OASFs irrespective of the stimulations. In contrast, the F2 score, which was a major *IL6* producer in the sublining, was strongly upregulated under IFN-γ, IFN-α, IL-6 or 8-mix stimulation. Accordingly, we surmised that certain SF populations were quantitatively stable between the diseases, and some are inducible under inflammation.

eQTL effects of RA risk loci are modulated by an environmental perturbation

We next performed cis-eQTL analysis to evaluate the effect of genetic variants on gene expressions. Together with tissue-by-tissue analysis, we also utilized Meta-Tissue software (online supplementary materials) for a meta-analysis across SFs under 10 stimulations and 5 PBMC subsets. When we analyzed RA and OA samples separately, the eQTL effect sizes showed high similarities between the diseases. To improve analytical ability, we jointly analyzed the RA and OA samples. We considered variants with FDR < 0.1 in single tissue analysis or *m*-value > 0.9 in meta-analysis as significant eQTLs.[14, 15]

As a result, 3245 - 4118 genes in SFs and 2557 - 2828 genes in PBMCs had significant eQTLs. In total, 2368 genes showed eQTL effects only in SFs (online supplementary figure 2A,B). A tissue-wise difference of eQTL effects was indicated by a distinguishable pattern of eQTLs in SFs from that of PBMCs when comparing the effect sizes in meta-analysis (online supplementary figure 2C).

When we focused on stimulated SFs, the 8-mix showed the smallest correlation coefficients compared with other conditions.

Furthermore, we examined candidate causal genes among RA risk loci in SFs. We focused on eQTL variants with minimum *P* values in each associated eGene with meta-analysis or single tissue analysis, which are in linkage disequilibrium (LD) with GWAS top-associated loci (online supplementary table 1). One example is rs6074022, which is in tight LD (r^2 = 0.95 in EUR, r^2 = 0.9 in EAS population) with an established RA risk SNP rs4810485.[16] rs6074022 had robust eQTL effects on *CD40* in SFs, especially under 8-mix or IFN-γ stimulations (figure 3A,D). Importantly, the presence of an active regulatory region at rs6074022 was inferred only under these conditions (figure 3B). Although *CD40* is also expressed by B cells (figure 3C), the eQTL effect was not observed at this locus (figure 3D).

The biological role of the CD40-CD40L pathway in SFs has been discussed.[17, 18] We performed transcriptomic analysis of RASFs stimulated with a 2-trimer form of the CD40 ligand and IFN-γ. As a result, some cytokines (e.g., *IL6*) and chemokines (e.g., *CCL5*, *CXCL10*) were significantly upregulated by the ligation of CD40L (figure 3E). Taken together, we conjecture that CD40 expression in SFs is influenced by genetic and environmental predisposition, and the CD40-CD40L pathway might have a pathogenic role in RASFs. Other examples of eQTL-eGene pairs in SFs are shown in online supplementary figure 3.

Genetic risk of RA accumulate in the transcriptomic and epigenomic perturbations induced by synergistic proinflammatory cytokines

Next, in order to elucidate the link between RA genetic risk and transcriptomic perturbations of activated SFs, we performed gene-set enrichment analysis with RA risk loci using MAGMA software (online supplementary materials). This analysis indicated that perturbed gene sets subject to IFN-α, IFN-γ and 8-mix stimulation significantly overlapped with RA risk loci ($P = 2.0 \times 10^{-4}$, 1.7×10^{-4} and 8.3×10^{-6}, respectively) (online supplementary figure 4A,B). Those data contrasted with the non-significant association of transcriptome differences between the diseases with RA genetic risk. These findings indicate that there is an accumulation of RA genetic risk in the pathways that are perturbed under specific conditions in SFs.

We also assessed the enrichment of GWAS top-associated loci in regulatory regions including super-enhancers (SEs). SEs are large clusters of enhancers collectively bound by an array of transcription factors (TFs) to define cell identity, and are hotspots for disease susceptibility.[19-21] Although the significant overlap of SEs in Th cells and B cells with RA risk loci has been reported,[19] SFs have not been examined. Here we compared the enrichment of RA risk loci to SEs and typical-enhancers (TEs), and risk loci showed significant enrichment with SEs in $CD4^+$ T cells and B cells, as well as with SEs in 8-mix stimulated SFs (figure 4A). Some risk loci showed overlap

with SEs which appear uniquely under 8 mix treatment (figure 4B,C). When we performed a similar analysis using risk loci for type 1 diabetes mellitus (a representative non-articular autoimmune disease), only SEs in $CD4^+$ T cells and B cells showed significant enrichment (online supplementary figure 4C). The number or width of 8-mix SEs were comparable to those in other stimulations (online supplementary figure 5). Consequently, SFs might behave as key players in RA pathogenesis especially under synergistic inflammation.

SEs induced by cytokine mixtures regulate genes crucial for RA pathogenesis

Following the results above, we attempted to elucidate the genes regulated by 8-mix-enhanced SEs. First, we combined the 3D genome architectures (chromatin loops detected by Hi-C analysis), the position of SEs, promoter regions (defined with H3K4me3 ChIP sequencing analysis) and genomic coordinates. We annotated "SE-contacted genes" such that one side of Hi-C loop anchors overlapped a SE, the other side coincided with the TSS and coexisted with the H3K4me3 peak (figure 5A). SEs were highly overlapped with Hi-C loop anchors than were TEs or H3K4me1 peaks (online supplementary figure 6A). When the TSS and H3K27ac peak was connected by a Hi-C loop, the variation of mRNA expression showed a significant correlation with the H3K27ac peak variation (online supplementary figure 6B). These results underscore the validity of connecting active enhancer marks and TSS by Hi-C loops as previous reports.[22, 23] When we compared the

expression of SE-contacted genes and TE-contacted genes, the former showed significantly higher expression than the latter (online supplementary figure 6C).[21]

Next, we compared genes contacted by either SEs or TEs of SFs under 3 different conditions: non-stimulated, TNF-α or the 8-mix. The proportions of overlap between these conditions were smaller in SE-contacted genes (9.7%) than TE-contacted genes (14.5%) (figure 5B), indicating that the stimulation-specific expression profile and SEs formation. SE-contacted genes included a number of TFs (e.g., *MTF1*, *RUNX1*), cytokines (e.g., IL6) and chemokines (e.g., *CCL5*, *CCL8*) (figure 5B, online supplementary table 2).

IL6 is a representative example of an 8-mix SE-contacted gene. Although this gene is regulated by a SE (almost 30 kb long) that exists upstream of the TSS in non-stimulated or TNF-α stimulated SFs, this SE elongates to 70 kb long under the 8-mix and an additional Hi-C loop emerges (figure 6A). When we inhibited SE formation with JQ1, a BRD4 inhibitor, the increased IL-6 expression under the 8-mix was disturbed (figure 6B). The necessity of SEs for elevated IL-6 production under synergistic inflammation was inferred.

Another example is *Runt related transcription factor 1* (*RUNX1*), a master-regulator involved in normal and malignant hematopoiesis.[24-26] The binding motif of *RUNX1* was enriched in SEs of synovial fluid-derived $CD4^+$ T cells from juvenile idiopathic arthritis patients.[27] In our study, RA risk locus rs8133843 overlapped with an 8-mix SE that exists upstream of *RUNX1* (figure 6C). A Hi-

C loop was formed with the promoter immediately above the second exon of *RUNX1* only in the 8-mix, and the *RUNX1* expression was higher in the 8-mix compared with others (figure 6D).

Metal-regulatory transcription factor-1 (*MTF1*), a zinc finger TFs, is another example. RA risk locus rs28411352 overlapped with an 8-mix unique SE that exists upstream of the *MTF1* (figure 6E). The Hi-C loop was detected with the promoter only under the 8-mix. *MTF1* expression was upregulated in the 8-mix (figure 6F).

Transcription factors associated with stimulation-induced SE formation control arthritis progression

Finally, we searched for candidate modulators that were crucial for SE formation, especially in the 8-mix. In the previous study, key TFs for SE formation were reported to be controlled by SEs themselves, forming a self-regulatory network.[21] From this perspective, we used motif analysis to focus on SE-contacted TFs that were also enriched in 8-mix SEs and compared them with TEs or unstimulated SEs (figure 7A). Among SE-contacted genes, TFs such as SNAI1, TCF4 and MTF1 showed significant motif enrichment in 8-mix SEs. MTF1 was the only example that also showed the overlap of 8-mix SE and RA risk variant (figure 6E). Although the RUNX1 motif was not enriched in 8-mix SEs compared with unstimulated SEs, its motif was significantly enriched in SEs compared with the background sequence, both in 8-mix and without stimulation ($P = 1.0 \times 10^{-16}$ and

1.0×10^{-20}, respectively). *In vitro* validation analysis showed that the expression of 8-mix SE-contacted genes was significantly suppressed by *MTF1* and *RUNX1* knockdown ($P = 2.0 \times 10^{-3}$ and 4.3×10^{-4}, respectively) (figure 7B, online supplementary figure 7). The effect of *MTF1* knockdown was more pronounced in 8-mix SE-contacted genes than TE-contacted genes. In *in vitro* assay, the increased 8-mix SE-contacted gene expressions (IL-6, CCL5) from stimulated RASFs was reduced by treatment with APTO-253, a MTF1 inhibitor (figure 7C,D).[28] Furthermore, in a collagen induced arthritis (CIA) model, APTO-253 demonstrated significant preventive (online supplementary figure 8) and therapeutic activity (figure 7E,F) on arthritis formation. Collectively, these results indicated that certain TFs play critical roles in the formation of epigenomic structures induced by synergistic proinflammatory cytokines, and support MTF1 inhibition as a promising therapy candidate for RA (online supplementary figure 9).

Discussion

In this study, we were able to describe the dynamic landscape of activated SFs and their contribution to RA pathogenesis. Recent large-scale eQTL studies enhanced our understanding of complex diseases.[29, 30] Considering the importance of studying disease-relevant tissues for functional understanding of GWAS variants,[14, 31] we conducted cis-eQTL analysis of SFs, which are major local effector cells in arthritic joints. One example of eQTL-eGene pairs in SFs was the association

of an RA risk SNP (rs4810485) with *CD40* expression. Although no significant eQTL effects of this locus in B cells was observed in our data, a previous report showed the protein-level QTL association of CD40 in $CD19^+$ B cells and this locus in Europeans.[32] On the contrary, a larger eQTL study by the GTEx consortium that showed genome-wide significant eQTL effects of rs6074022 on CD40 in lung (mainly fibroblasts) ($P = 3.1 \times 10^{-26}$) and cultured fibroblasts ($P = 8.4 \times 10^{-16}$), but not in EBV-transformed lymphocytes ($P = 0.04$).[33] The subtle gap in results could be derived from racial differences of study populations and study design. Naturally, although the possible importance of CD40 signals in B cells for RA pathogenesis cannot be neglected, our result shed light on the role of CD40-CD40L signals in a genetic network of synovitis.

The significance of synergistic interactions between proinflammatory cytokines and SFs is supported by the observed accumulation of RA risk loci as shown by transcriptomic and epigenomic data. The GWAS-SEs enrichment analysis shows that SFs can behave as pathogenic cells in the development of RA (analogous to $CD4^+$ T cells and B cells) especially when exposed to the synergistically acting cytokines. Furthermore, recent fine chromatin contact maps revealed that SEs are in close proximity to the promoter of the gene they activate.[34-37] During cytokine synergy, Hi-C analysis suggested that there were dynamic conformational changes in three-dimensional structures involving SEs and the promoter of pathological molecules. We found marked expression of 8-mix stimulated SE-contacted genes (i.e., *IL6*, *RUNX1*, *MTF1*).

SEs can collapse when their co-factors (e.g., BET family) are perturbed.[38] In RASFs, BRD4 silencing or inhibitor reduced cytokine secretion, migration and invasion activity, and ameliorated experimental arthritis.[39] On the other hand, selective modulation of disease-associated SEs in a cell type-specific manner may have better safety profiles than pan-SEs inhibitors (i.e., JQ1). In T cell leukemias, a small monoallelic insertion creates binding motifs for the master regulator MYB, which trigger SEs initiation upstream of oncogenes.[25] In the present study, we analyzed TFs that have the potential to be selective SE modulators in activated SFs. Our results suggested that MTF1 participates in SE formation, putatively making a feedback loop to maintain the epigenomic machinery. MTF1 regulates gene expression in response to zinc and various stresses.[40] In the setting of disease, MTF1 could contribute to tumor metastasis and chemoresistance in some cancer cells.[41] APTO-253, a MTF1 inhibitor,[28] is a small molecule with antitumor activity against a wide range of human malignancies in *in vitro* and *in vivo*.[42, 43] In the present study, APTO-253 demonstrated inhibitory activity on the expression of pathogenic molecules (IL-6, CCL5) from RASFs and antiarthritic activity in a CIA model. Previously, the zinc-ZIP8-MTF1 axis was identified as a catabolic regulator of cartilage destruction.[44] Furthermore, intra-articular injection of adenovirus expressing-MTF1 in an experimental mouse model of OA promoted the expression of various matrix-degrading enzymes, cytokines and chemokines in SFs. This evidence supports the essential role of MTF1 as a genetic hub for joint destruction and inflammation.

There are some limitations of this study. First, the number of patients included in the cis-eQTL analysis was limited owing to sample accessibility, resulting in putatively large false negatives. Second, SFs were purified by serial passages. Previous reports showed that passage number could affect the epigenome and transcriptome of SFs.[45, 46] To minimize the impact of culture, we restricted our analysis to early passage cells. Third, isolated PBMCs were not artificially stimulated with cytokines *ex vivo*. Thus, it is not clear whether the eQTL difference between SFs and PBMCs is attributable to cell type difference. However, over 80% of RA patients had moderate to high disease activity at the time of blood sampling, indicating that PBMCs were subject to a proinflammatory environment.

Overall, our findings shed light on the concept of SF-targeted therapy from the perspective of epigenome remodeling. Some TFs (MTF1, RUNX1) preferentially recruited to SEs during exposure to synergistic proinflammatory cytokines would constitute novel drug targets.

Acknowledgments:

We would like to thank G Inoue, M Abe, K Myouzen and K Kobayashi for their technical assistance at the Laboratory for Autoimmune Diseases, and Dr. Y Momozawa and Dr. M Kubo for providing technical advice at the Laboratory for Genotyping Development, RIKEN. We received generous support from all the physicians who participated in sample collection at the Department of Orthopaedic Surgery, the University of Tokyo. **Funding**: This research was supported by funding from Takeda Pharmaceutical Co., Ltd. (Y. Kochi., K. Y. and K.F.), the Ministry of Health, Labour and Welfare, Ministry of Education, Culture, Sports, Science and Technology KAKENHI Grant-in-Aid for Scientific Research (B) (18H02846) and Grant-in-Aid for Scientific Research (C) (17K09972) from the Japan Society for the Promotion of Science. **Author contributions**: H.T., S.S., K.I., Y. Kochi., K.Y. and K.F. designed the research project. M.O. conducted bioinformatics analysis on the advice of K.I.. A.S. performed RNA sequencing. H.T. performed ChIP sequencing and other in vitro experiments. T.S. and K.S. performed Hi-C. H.T., Y.T., H.I., J.H., Y. Kadono. and S.T. contributed human samples. S.S. performed figure editing. H.T. and M.O. wrote the manuscript with critical inputs from Y. Kochi., K.Y. and K.F.. **Competing interests**: None declared. **Data and materials availability**: The datasets generated during this study are available at the National Bioscience Database Center (NBDC) with the study accession code hum0207 (read counts data of

RNA sequencing, hum0207.v1.RNA.v1; eQTL summary, hum0207.v1.eQTL.v1; peaks data of ChIP sequencing, hum0207.v1.ChIP.v1; chromatin loops data of Hi-C, hum0207.v1.HiC.v1).

References:

1 van Vollenhoven R. Treat-to-target in rheumatoid arthritis - are we there yet? *Nature reviews Rheumatology* 2019;15:180-6.

2 Baker KF, Isaacs JD. Novel therapies for immune-mediated inflammatory diseases: What can we learn from their use in rheumatoid arthritis, spondyloarthritis, systemic lupus erythematosus, psoriasis, Crohn's disease and ulcerative colitis? *Annals of the rheumatic diseases* 2018;77:175-87.

3 Chen Z, Bozec A, Ramming A, et al. Anti-inflammatory and immune-regulatory cytokines in rheumatoid arthritis. *Nature reviews Rheumatology* 2019;15:9-17.

4 Okada Y, Wu D, Trynka G, et al. Genetics of rheumatoid arthritis contributes to biology and drug discovery. *Nature* 2014;506:376-81.

5 Farh KK, Marson A, Zhu J, et al. Genetic and epigenetic fine mapping of causal autoimmune disease variants. *Nature* 2015;518:337-43.

6 Fairfax BP, Humburg P, Makino S, et al. Innate immune activity conditions the effect of regulatory variants upon monocyte gene expression. *Science (New York, NY)* 2014;343:1246949.

7 Ai R, Laragione T, Hammaker D, et al. Comprehensive epigenetic landscape of rheumatoid arthritis fibroblast-like synoviocytes. *Nature communications* 2018;9:1921.

8 Slowikowski K, Wei K, Brenner MB, et al. Functional genomics of stromal cells in chronic inflammatory diseases. *Current opinion in rheumatology* 2018;30:65-71.

9 Leech MT, Morand EF. Fibroblasts and synovial immunity. *Current opinion in pharmacology* 2013;13:565-9.

10 Katz Y, Nadiv O, Beer Y. Interleukin-17 enhances tumor necrosis factor alpha-induced synthesis of interleukins 1,6, and 8 in skin and synovial fibroblasts: a possible role as a "fine-tuning cytokine" in inflammation processes. *Arthritis and rheumatism* 2001;44:2176-84.

11 Arend WP, Dayer JM. Cytokines and cytokine inhibitors or antagonists in rheumatoid arthritis. *Arthritis and rheumatism* 1990;33:305-15.

12 Zhang F, Wei K, Slowikowski K, et al. Defining inflammatory cell states in rheumatoid arthritis joint synovial tissues by integrating single-cell transcriptomics and mass cytometry. *Nature immunology* 2019;20:928-42.

13 Hanzelmann S, Castelo R, Guinney J. GSVA: gene set variation analysis for microarray and RNA-seq data. *BMC bioinformatics* 2013;14:7.

14 Gamazon ER, Segre AV, van de Bunt M, et al. Using an atlas of gene regulation across 44 human tissues to inform complex disease- and trait-associated variation. *Nature genetics* 2018;50:956-67.

15 Sul JH, Han B, Ye C, et al. Effectively identifying eQTLs from multiple tissues by combining mixed model and meta-analytic approaches. *PLoS genetics* 2013;9:e1003491.

16 Raychaudhuri S, Remmers EF, Lee AT, et al. Common variants at CD40 and other loci

confer risk of rheumatoid arthritis. *Nature genetics* 2008;40:1216-23.

17 Cho ML, Yoon BY, Ju JH, et al. Expression of CCR2A, an isoform of MCP-1 receptor, is increased by MCP-1, CD40 ligand and TGF-beta in fibroblast like synoviocytes of patients with RA. *Experimental & molecular medicine* 2007;39:499-507.

18 Kim KW, Cho ML, Kim HR, et al. Up-regulation of stromal cell-derived factor 1 (CXCL12) production in rheumatoid synovial fibroblasts through interactions with T lymphocytes: role of interleukin-17 and CD40L-CD40 interaction. *Arthritis and rheumatism* 2007;56:1076-86.

19 Hnisz D, Abraham BJ, Lee TI, et al. Super-enhancers in the control of cell identity and disease. *Cell* 2013;155:934-47.

20 Kundaje A, Meuleman W, Ernst J, et al. Integrative analysis of 111 reference human epigenomes. *Nature* 2015;518:317-30.

21 Whyte WA, Orlando DA, Hnisz D, et al. Master transcription factors and mediator establish super-enhancers at key cell identity genes. *Cell* 2013;153:307-19.

22 Delaneau O, Zazhytska M, Borel C, et al. Chromatin three-dimensional interactions mediate genetic effects on gene expression. *Science (New York, NY)* 2019;364.

23 Mumbach MR, Satpathy AT, Boyle EA, et al. Enhancer connectome in primary human cells identifies target genes of disease-associated DNA elements. *Nature genetics* 2017;49:1602-12.

24 Bahr C, von Paleske L, Uslu VV, et al. A Myc enhancer cluster regulates normal and

leukaemic haematopoietic stem cell hierarchies. *Nature* 2018;553:515-20.

25 Mansour MR, Abraham BJ, Anders L, et al. Oncogene regulation. An oncogenic super-enhancer formed through somatic mutation of a noncoding intergenic element. *Science (New York, NY)* 2014;346:1373-7.

26 Mill CP, Fiskus W, DiNardo CD, et al. RUNX1-targeted therapy for AML expressing somatic or germline mutation in RUNX1. *Blood* 2019;134:59-73.

27 Peeters JG, Vervoort SJ, Tan SC, et al. Inhibition of Super-Enhancer Activity in Autoinflammatory Site-Derived T Cells Reduces Disease-Associated Gene Expression. *Cell reports* 2015;12:1986-96.

28 Osmanbeyoglu HU, Shimizu F, Rynne-Vidal A, et al. Chromatin-informed inference of transcriptional programs in gynecologic and basal breast cancers. *Nature communications* 2019;10:4369.

29 Battle A, Brown CD, Engelhardt BE, et al. Genetic effects on gene expression across human tissues. *Nature* 2017;550:204-13.

30 Lappalainen T, Sammeth M, Friedlander MR, et al. Transcriptome and genome sequencing uncovers functional variation in humans. *Nature* 2013;501:506-11.

31 Wainberg M, Sinnott-Armstrong N, Mancuso N, et al. Opportunities and challenges for transcriptome-wide association studies. *Nature genetics* 2019;51:592-9.

32 Li G, Diogo D, Wu D, et al. Human genetics in rheumatoid arthritis guides a high-throughput drug screen of the CD40 signaling pathway. *PLoS genetics* 2013;9:e1003487.

33 The GTEx consortium. https://www.gtexportal.org/home/

34 Dowen JM, Fan ZP, Hnisz D, et al. Control of cell identity genes occurs in insulated neighborhoods in mammalian chromosomes. *Cell* 2014;159:374-87.

35 Hnisz D, Weintraub AS, Day DS, et al. Activation of proto-oncogenes by disruption of chromosome neighborhoods. *Science (New York, NY)* 2016;351:1454-8.

36 Ji X, Dadon DB, Powell BE, et al. 3D Chromosome Regulatory Landscape of Human Pluripotent Cells. *Cell stem cell* 2016;18:262-75.

37 Kieffer-Kwon KR, Tang Z, Mathe E, et al. Interactome maps of mouse gene regulatory domains reveal basic principles of transcriptional regulation. *Cell* 2013;155:1507-20.

38 Loven J, Hoke HA, Lin CY, et al. Selective inhibition of tumor oncogenes by disruption of super-enhancers. *Cell* 2013;153:320-34.

39 Zhang QG, Qian J, Zhu YC. Targeting bromodomain-containing protein 4 (BRD4) benefits rheumatoid arthritis. *Immunology letters* 2015;166:103-8.

40 Gunther V, Lindert U, Schaffner W. The taste of heavy metals: gene regulation by MTF-1. *Biochimica et biophysica acta* 2012;1823:1416-25.

41 Ji L, Zhao G, Zhang P, et al. Knockout of MTF1 Inhibits the Epithelial to Mesenchymal

Transition in Ovarian Cancer Cells. *Journal of Cancer* 2018;9:4578-85.

42 Local A, Zhang H, Benbatoul KD, et al. APTO-253 Stabilizes G-quadruplex DNA, Inhibits MYC Expression, and Induces DNA Damage in Acute Myeloid Leukemia Cells. *Molecular cancer therapeutics* 2018;17:1177-86.

43 Tsai CY, Sun S, Zhang H, et al. APTO-253 Is a New Addition to the Repertoire of Drugs that Can Exploit DNA BRCA1/2 Deficiency. *Molecular cancer therapeutics* 2018;17:1167-76.

44 Kim JH, Jeon J, Shin M, et al. Regulation of the catabolic cascade in osteoarthritis by the zinc-ZIP8-MTF1 axis. *Cell* 2014;156:730-43.

45 Galligan CL, Baig E, Bykerk V, et al. Distinctive gene expression signatures in rheumatoid arthritis synovial tissue fibroblast cells: correlates with disease activity. *Genes and immunity* 2007;8:480-91.

46 Whitaker JW, Shoemaker R, Boyle DL, et al. An imprinted rheumatoid arthritis methylome signature reflects pathogenic phenotype. *Genome medicine* 2013;5:40.

Figure legends:

Figure 1. Experimental design for integrative analysis of activated SFs from RA and OA patients.

Our study design included SFs stimulated by 8 different factors plus a combination of all the factors. Specifically, cells were treated for 24 h with one of the following: IFN-α 100 U/mL, IFN-γ 200 U/mL, TNF-α 10 ng/mL, IL-1β 10 ng/mL, IL-6/sIL-6R 200 ng/mL, IL-17 10 ng/mL, TGF-β1 10 ng/mL or IL-18 100 ng/mL or 8-mix, a mixture of the above 8 cytokines. In addition, we used 5 freshly isolated PBMC populations ($CD4^+$ T cells, $CD8^+$ T cells, B cells, NK cells, monocytes) from the same patient cohort. RNA sequencing of individual samples from RA and OA patients (n=30 per each) was carried out, and ChIP sequencing and Hi-C analysis were conducted with pooled samples. SNP genotyping array was performed in all patients.

SFs, synovial fibroblasts; PBMCs, peripheral blood mononuclear cells; RA, rheumatoid arthritis; OA, osteoarthritis; NS, non-stimulated.

Figure 2. A distinctive transcriptome signature in SFs induced by the mixture of 8 cytokines.

(**A**) Principal Component Analysis (PCA) of gene expression levels for the top 1000 variable genes. Samples projected onto PC1/PC2 (left) or PC3/PC4 (right). Numbers in parentheses indicate contribution ratio (percentage of variation) of the first 4 PCs. Arrows link the centroid of indicated groups and adjusted to start from the origin.

(**B**) Summary of PCA for top 1000 variable genes. We fit a linear model to each PC (i.e., PC ~ Disease + Stimulation). Then we transformed the *P* values to normal Z-scores.

(**C**) Transcript abundances of representative RA pathogenic genes (*IL6*, *MMP3* and *CSF2*) from RNA sequencing data in stimulated SFs. Boxes, interquartile range; whiskers, distribution; dots, outliers.

PCA, principal component analysis; RA, rheumatoid arthritis; OA, osteoarthritis; NS, non-stimulated; CPM, count per million.

Figure 3. Stimulation-specific function of RA genetic risk loci.

(**A**) A dot plot of rs6074022-*CD40* cis-eQTL meta-analysis posterior probability *m*-values versus tissue-by-tissue analysis -$\log_{10}$ *P* value. The gray solid line (*m*-value = 0.9) corresponds to the significance threshold in this study.

(**B**) Transcriptional regulatory regions around the *CD40* gene and positional relationship of rs6074022 (blue triangle) in stimulated SFs and PBMCs. IRF1 biding sites were obtained from the public epigenome browser ChIP-Atras. Data were visualized using the Integrative Genomics Viewer (IGV).

(**C**) Transcript abundance of *CD40* from RNA sequencing data in stimulated SFs and PBMCs.

(**D**) Expression of *CD40* in SFs stimulated by the mixture of 8 cytokines (left) and B cells (right) from each individual plotted according to the rs6074022 genotype. Nominal *P* values in eQTL mapping are shown.

(**E**) A volcano plot of differential gene expression analysis comparing the presence or absence of CD40 ligand (CD40L) for IFN-γ-stimulated SFs. Orange and blue points mark the genes with significantly increased or decreased expression respectively for the addition of CD40L (FDR <0.01).

Boxes, interquartile range; whiskers, distribution; dots, outliers in (**C**) and (**D**).

RA, rheumatoid arthritis; OA, osteoarthritis; NS, non-stimulated; CPM, count per million.

Figure 4. Enrichment of RA genetic risk in SFs super-enhancers under 8 cytokine stimulation.

(**A**) Enrichment of RA risk loci in transcriptional regulatory regions of stimulated SFs and PBMCs. Active enhancers were classified into super-enhancers (SEs) and typical-enhancers (TEs) following standard ROSE algorithms. The red solid lines ($-\log_{10}$ (*P* value) = 3.2) and the black solid lines ($-\log_{10}$ (*P* value) = 1.3) are the cutoffs for Bonferroni significance and nominal *P* = 0.05, respectively.

(**B**) A circus plot showing the overlap of SEs in SFs under different stimulatory conditions. Only the regions unique to each condition or common to all of the conditions are depicted.

(**C**) A circus plot showing the overlap of RA risk loci and SEs in SFs under different stimulatory conditions.

NS, non-stimulated; SE, super-enhancer; TE, typical enhancer.

Figure 5. RA pathogenic factors regulated by SEs in SFs treated with 8 cytokines.

(**A**) A schematic image of “SE-contacted genes”.

(**B**) A Venn diagram representing the overlap of TE-contacted (top) or SE-contacted (bottom) genes in SFs under different stimulatory conditions. Red, blue and black text highlight genes whose contacted SEs overlap with RA risk loci, cytokines and chemokines and transcription factors, respectively.

TSS, transcriptional start site; NS, non-stimulated; SE, super-enhancer; TE, typical enhancer.

Figure 6. Representative SE-contacted genes in SFs treated with 8 cytokines.

(**A, C, E**) Organization of transcriptional regulatory regions around *IL6* (**A**), *RUNX1* (**C**) and *MTF1* (**E**) genes and positional relationship of RA risk loci (blue triangle, rs8133848 for *RUNX1* and rs28411352 for *MTF1*) and chromatin conformation in stimulated SFs. Data were visualized using the Integrative Genomics Viewer (IGV).

(**B**) Expression of IL-6 in SFs treated with JQ1. The mRNA and protein expression were quantified by qRT-PCR (left) and ELISA (right), respectively. Bar graphs, mean; Error bars, SEM. *P* values were determined using one-way ANOVA followed by Tukey's multiple comparison test (*, $P < 0.05$, ***, $P < 0.001$).

(**D, F**) Transcript abundances of *RUNX1* isoform (RUNX1b) (**D**) and *MTF1* (**F**) from RNA sequencing data for stimulated SFs and PBMCs. Boxes, interquartile range; whiskers, distribution; dots, outliers. RA, rheumatoid arthritis; OA, osteoarthritis; NS, non-stimulated; TPM, transcripts per million; CPM, count per million; SE, super enhancer.

Figure 7. Transcription factors associated with stimulation-induced SE formation and arthritis progression.

(**A**) Table depicts transcription factor binding motifs enriched at SEs in stimulated SFs. Following are summarized: attribution to SE-contacted genes, relative enrichment *P* values to TEs in each stimulatory condition or to SEs of non-stimulated condition.

(**B**) Expression of SE- or TE-contacted genes in SFs stimulated by 8 cytokines in cells depleted of specified transcription factors (*TCF4*, *SNAI1*, *MTF1* and *RUNX1*) relative to control SFs. Boxes, interquartile range; whiskers, distribution. *P* values, paired t test (*, $P < 0.05$, ***, $P < 0.001$).

(**C, D**) Expression of IL-6 and CCL5 in SFs treated with APTO-253. The mRNA and protein level were quantified by qRT-PCR (**C**) and ELISA (**D**), respectively. Bar graphs, mean; Error bars, SEM. *P* values, one-way ANOVA followed by Tukey's multiple comparison test (*, $P < 0.05$, **, $P < 0.01$, ***, $P < 0.001$).

(**E, F**) Therapeutic effect of APTO-253 on CIA model. Following the onset of arthritis, mice were intravenously injected with either control or 15 mg/kg APTO-253 for twice per day for 2 consecutive days per week. Clinical (**E**) and pathological scores (**F**). Dots, mean; Error bars, SEM. *P* values, Mann–Whitney U test (*, $P < 0.05$, ***, $P < 0.001$).

NS, non-stimulated; SE, super enhancer; TE, typical enhancer.

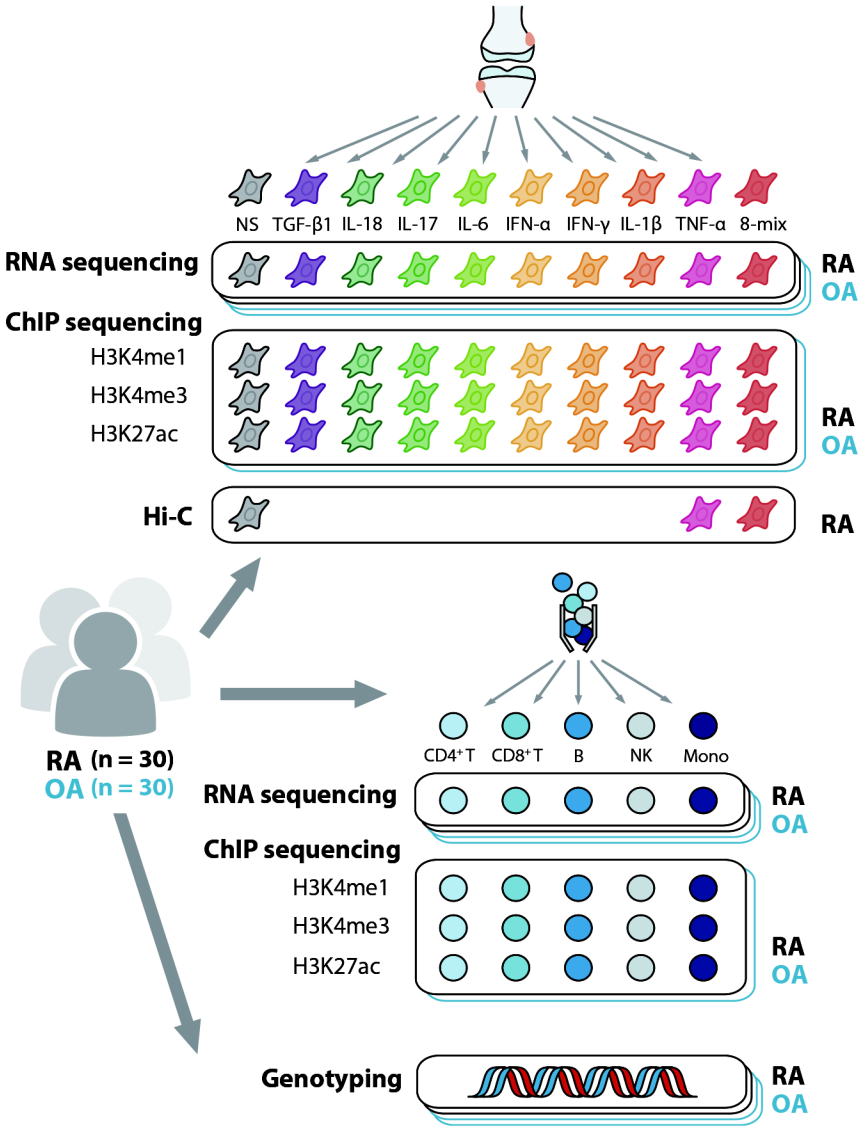
NS
TGF-β1
IL-18
IL-17
IL-6
IFN-α
IFN-γ
IL-1β
TNF-α
8-mix
RNA sequencing
RA
OA
ChIP sequencing
H3K4me1
H3K4me3
H3K27ac
RA
OA
Hi-C
RA
RA (n = 30)
OA (n = 30)
CD4+T
CD8+T
B
NK
Mono
RNA sequencing
RA
OA
ChIP sequencing
H3K4me1
H3K4me3
H3K27ac
RA
OA
Genotyping
RA
OA

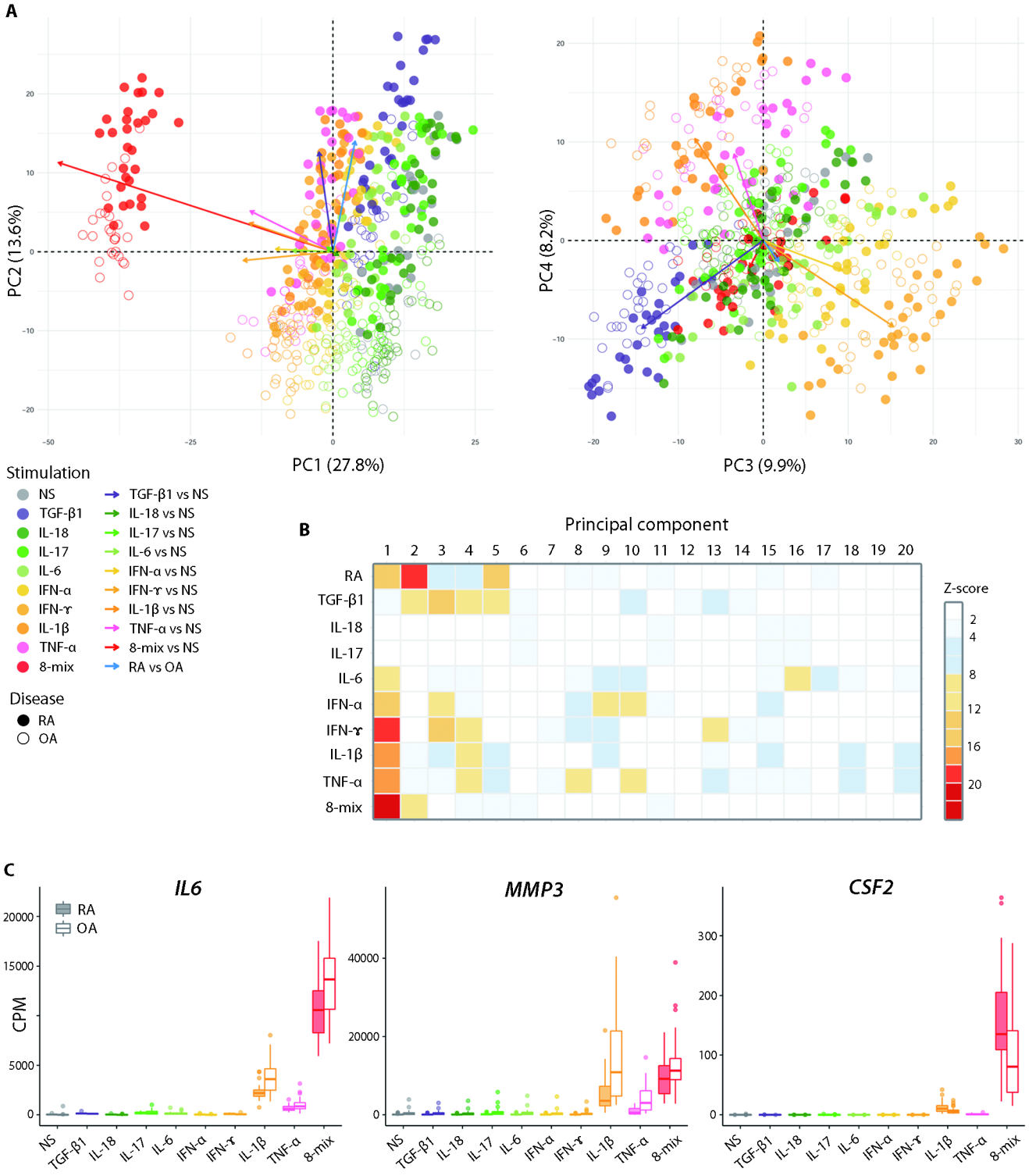
A
PC2 (13.6%)
PC1 (27.8%)
PC4 (8.2%)
PC3 (9.9%)
Stimulation
NS
TGF-β1
IL-18
IL-17
IL-6
IFN-α
IFN-γ
IL-1β
TNF-α
8-mix
TGF-β1 vs NS
IL-18 vs NS
IL-17 vs NS
IL-6 vs NS
IFN-α vs NS
IFN-γ vs NS
IL-1β vs NS
TNF-α vs NS
8-mix vs NS
RA vs OA
Disease
RA
OA
B
Principal component
Z-score
C
IL6
MMP3
CSF2
CPM
RA
OA

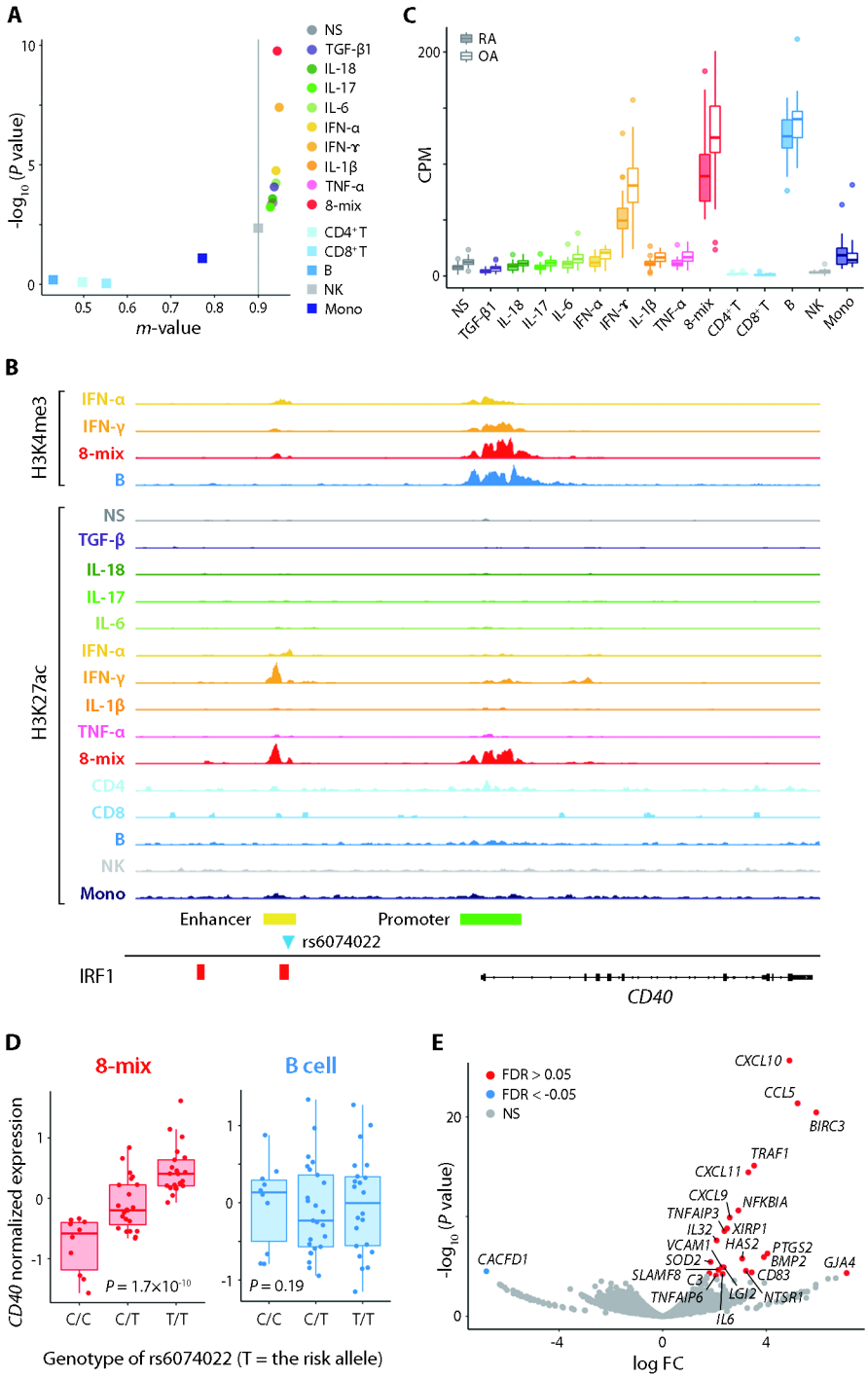
A
-log10 (P value)
m-value
NS
TGF-β1
IL-18
IL-17
IL-6
IFN-α
IFN-γ
IL-1β
TNF-α
8-mix
CD4+T
CD8+T
B
NK
Mono
C
RA
OA
CPM
B
H3K4me3
H3K27ac
Enhancer
Promoter
rs6074022
IRF1
CD40
D
8-mix
B cell
CD40 normalized expression
P = 1.7×10-10
P = 0.19
C/C
C/T
T/T
Genotype of rs6074022 (T = the risk allele)
E
FDR > 0.05
FDR < -0.05
NS
-log10 (P value)
log FC
CXCL10
CCL5
BIRC3
TRAF1
CXCL11
CXCL9
NFKBIA
TNFAIP3
IL32
XIRP1
VCAM1
HAS2
PTGS2
SOD2
BMP2
CACFD1
GJA4
SLAMF8
C3
CD83
TNFAIP6
LGI2
NTSR1
IL6

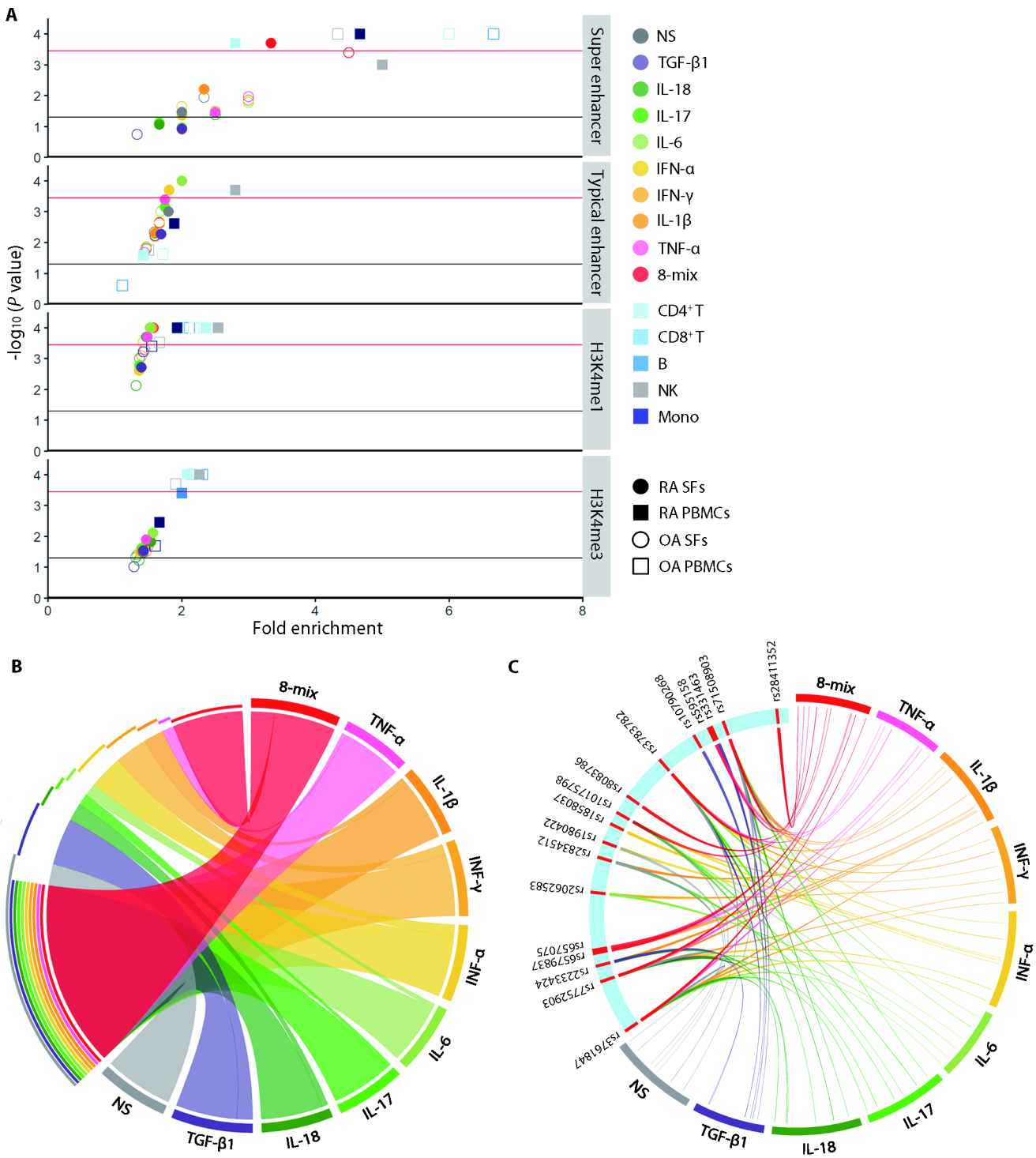
A
Super enhancer
Typical enhancer
H3K4me1
H3K4me3
-log10 (P value)
Fold enrichment
NS
TGF-β1
IL-18
IL-17
IL-6
IFN-α
IFN-γ
IL-1β
TNF-α
8-mix
CD4+T
CD8+T
B
NK
Mono
RA SFs
RA PBMCs
OA SFs
OA PBMCs
B
8-mix
TNF-α
IL-1β
INF-γ
INF-α
IL-6
IL-17
IL-18
TGF-β1
NS
C
rs28411352
rs71508903
rs531463
rs595158
rs1079026
rs3783782
rs8083786
rs1017579
rs1858037
rs1980422
rs2834512
rs2062583
rs657075
rs6579837
rs2233424
rs7752903
rs3761847

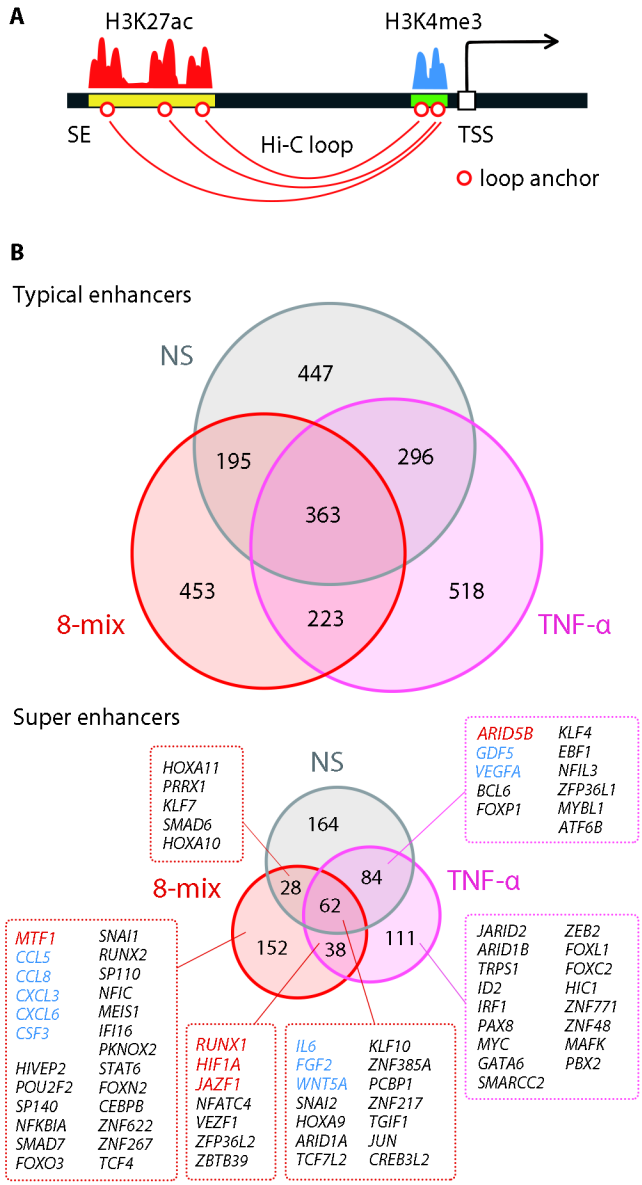
A
H3K27ac
H3K4me3
SE
Hi-C loop
TSS
loop anchor
B
Typical enhancers
NS
447
195
296
363
453
223
518
8-mix
TNF-α
Super enhancers
NS
164
8-mix
28
62
84
TNF-α
152
38
111
HOXA11
PRRX1
KLF7
SMAD6
HOXA10
ARID5B
GDF5
VEGFA
BCL6
FOXP1
KLF4
EBF1
NFIL3
ZFP36L1
MYBL1
ATF6B
MTF1
CCL5
CCL8
CXCL3
CXCL6
CSF3
HIVEP2
POU2F2
SP140
NFKBIA
SMAD7
FOXO3
SNAI1
RUNX2
SP110
NFIC
MEIS1
IFI16
PKNOX2
STAT6
FOXN2
CEBPB
ZNF622
ZNF267
TCF4
RUNX1
HIF1A
JAZF1
NFATC4
VEZF1
ZFP36L2
ZBTB39
IL6
FGF2
WNT5A
SNAI2
HOXA9
ARID1A
TCF7L2
KLF10
ZNF385A
PCBP1
ZNF217
TGIF1
JUN
CREB3L2
JARID2
ARID1B
TRPS1
ID2
IRF1
PAX8
MYC
GATA6
SMARCC2
ZEB2
FOXL1
FOXC2
HIC1
ZNF771
ZNF48
MAFK
PBX2

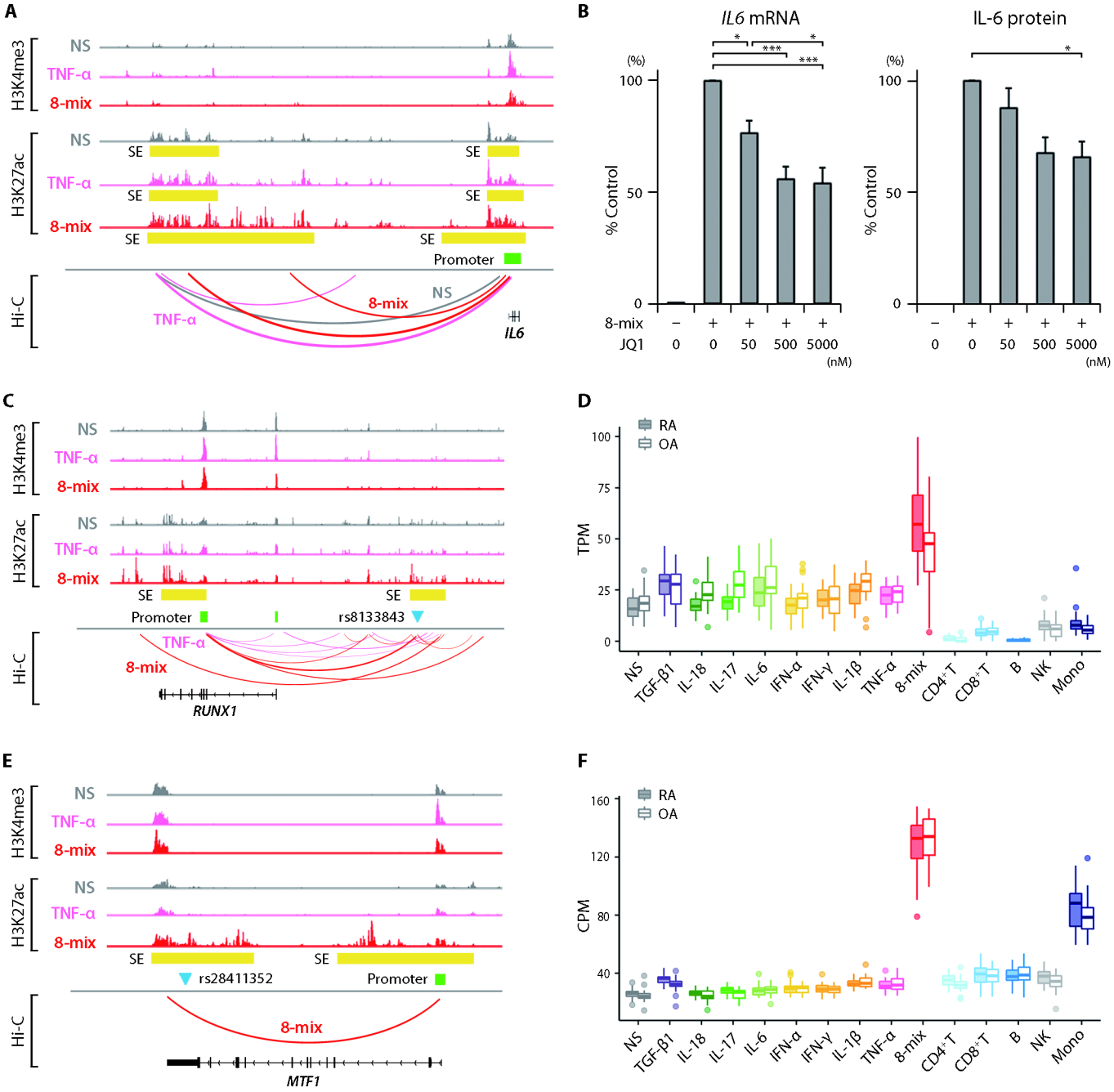
A
H3K4me3
NS
TNF-α
8-mix
H3K27ac
SE
Promoter
Hi-C
IL6
B
IL6 mRNA
IL-6 protein
(%)
% Control
8-mix
JQ1
(nM)
C
rs8133843
RUNX1
D
RA
OA
TPM
NS
TGF-β1
IL-18
IL-17
IL-6
IFN-α
IFN-γ
IL-1β
TNF-α
8-mix
CD4+T
CD8+T
B
NK
Mono
E
rs28411352
MTF1
F
CPM

A

TF	Motif	SEs enrichment *P* value							
		8-mix			TNF-α			NS	
		SEs-connection	vs TEs	vs NS SEs	SEs-connection	vs TEs	vs NS SEs	SEs-connection	vs TEs
SNAI1		yes	1.0×10^{-59}	1.0×10^{-14}	no	1.0×10^{-27}	> 0.05	no	1.0×10^{-45}
TCF4		yes	1.0×10^{-50}	1.0×10^{-13}	no	1.0×10^{-22}	> 0.05	no	1.0×10^{-40}
SNAI2		yes	1.0×10^{-48}	1.0×10^{-19}	yes	1.0×10^{-22}	> 0.05	yes	1.0×10^{-34}
MTF1		yes	1.0×10^{-18}	1.0×10^{-03}	no	1.0×10^{-05}	> 0.05	no	1.0×10^{-08}
SREBF1		no	1.0×10^{-09}	1.0×10^{-09}	yes	1.0×10^{-03}	> 0.05	no	1.0×10^{-04}
RARA		no	1.0×10^{-09}	1.0×10^{-08}	no	1.0×10^{-03}	1.0×10^{-06}	yes	1.0×10^{-05}
JUN		yes	1.0×10^{-03}	1.0×10^{-14}	yes	> 0.05	> 0.05	yes	1.0×10^{-03}
FOXL1	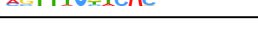	no	1.0×10^{-08}	1.0×10^{-04}	yes	1.0×10^{-04}	> 0.05	no	1.0×10^{-05}
ZNF740		no	1.0×10^{-07}	> 0.05	no	1.0×10^{-09}	1.0×10^{-02}	yes	1.0×10^{-17}
IRF1		no	> 0.05	1.0×10^{-33}	yes	> 0.05	> 0.05	no	> 0.05
CEBPB		yes	> 0.05	1.0×10^{-30}	no	> 0.05	1.0×10^{-06}	no	> 0.05

B

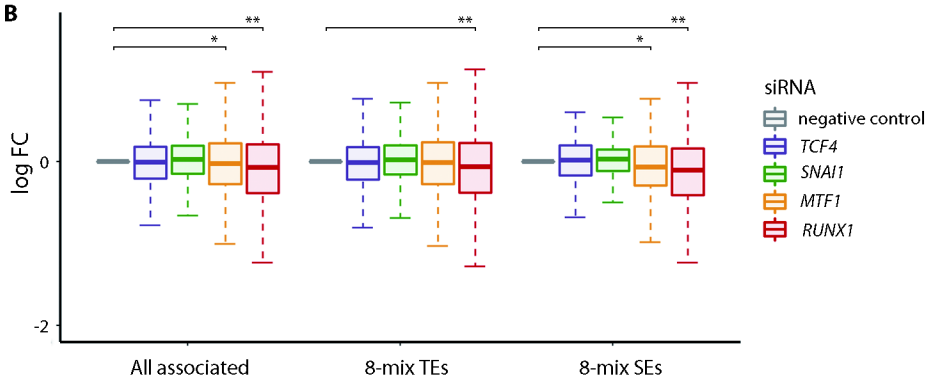

C

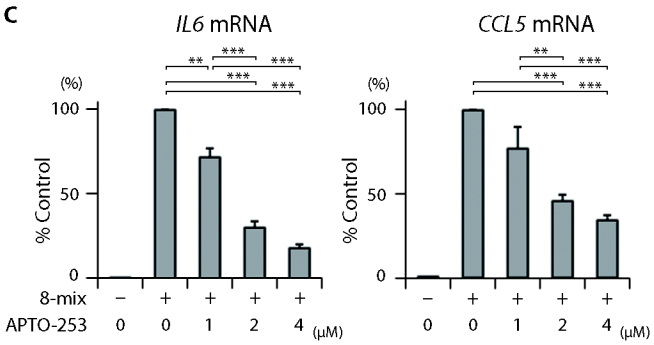

D

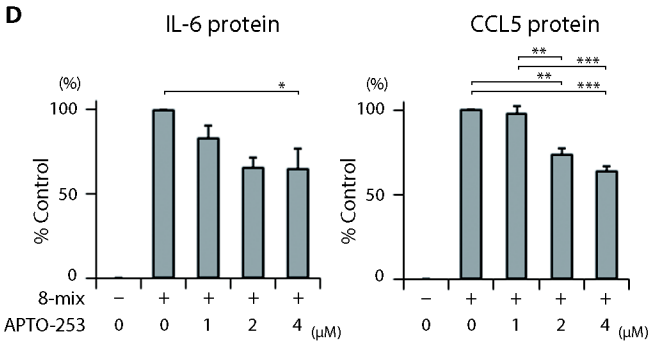

E

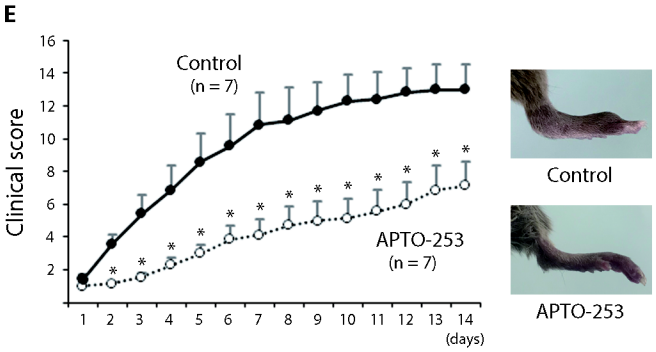
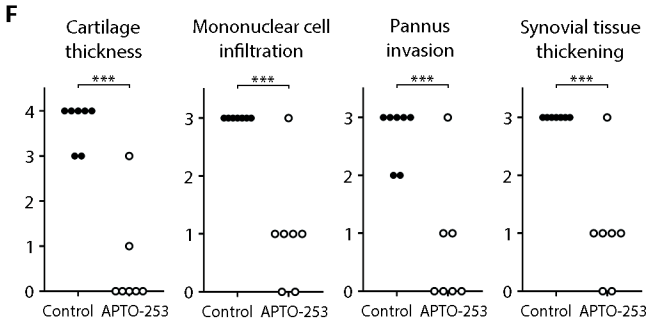
F